Intensity non-uniformity correction in MRI: Existing methods and their validation

Boubakeur Belaroussi [a,*], Julien Milles [b], Sabin Carme [c],
Yue Min Zhu [a], Hugues Benoit-Cattin [a]

[a] *CREATIS, UMR CNRS 5515, INSERM U 630, INSA Lyon, Bât. Blaise Pascal, 69621 Villeurbanne Cedex, France*
[b] *Division of Image Processing, Department of Radiology, Leiden University Medical Center, Leiden, The Netherlands*
[c] *Laboratoires Guerbet, Paris, France*

Abstract

Magnetic resonance imaging is a popular and powerful non-invasive imaging technique. Automated analysis has become mandatory to efficiently cope with the large amount of data generated using this modality. However, several artifacts, such as intensity non-uniformity, can degrade the quality of acquired data. Intensity non-uniformity consists in anatomically irrelevant intensity variation throughout data. It can be induced by the choice of the radio-frequency coil, the acquisition pulse sequence and by the nature and geometry of the sample itself. Numerous methods have been proposed to correct this artifact. In this paper, we propose an overview of existing methods. We first sort them according to their location in the acquisition/processing pipeline. Sorting is then refined based on the assumptions those methods rely on. Next, we present the validation protocols used to evaluate these different correction schemes both from a qualitative and a quantitative point of view. Finally, availability and usability of the presented methods is discussed.
© 2005 Elsevier B.V. All rights reserved.

Keywords: Magnetic resonance imaging; Intensity non-uniformity artifact; Image intensity correction; Validation methods

1. Introduction

Magnetic resonance imaging (MRI) is a powerful non-invasive imaging technique for studying soft tissues anatomy and properties. It is characterized by an overall good quality of obtained datasets. Such data usually consist of either a collection of two-dimensional (2-D) MR images or a whole three-dimensional (3-D) isotropic volume. Efficient qualitative or user-driven quantitative analysis can be performed on MR data, but current needs are non-supervised, automated, quantitative analysis tools.

MR datasets can be corrupted by several artifacts (Bellon et al., 1986), which affect automated quantitative analysis results. Some of those artifacts are directly related to the acquisition technique while others are linked to the imaged object itself. Corrupted datasets show distortions that may lead to a wrong quantification.

In this paper, we focus on the intensity non-uniformity artifact whose effects are shown in Fig. 1. Its main consequence is a slow and smooth intensity variation across datasets (Hanson and Dyrby, 2002). Most automated quantitative methods rely on the assumption that a given tissue is represented by similar voxel intensities throughout data. As a result quantitative parameters computed from corrupted data will likely be erroneous. Correcting or reducing the effects of this artifact is thus a crucial issue for the use of quantitative MRI analysis in daily clinical practice.

Intensity non-uniformity has no anatomical relevance and is mainly caused by unwanted local flip angle variations, but triggers for this variation can be multiple. A MR image is the result of the combination of an imaging

---

* Corresponding author. Tel.: +33 4 72 43 64 70; fax: +33 4 72 43 63 12.
 E-mail address: boubakeur.belaroussi@creatis.insa-lyon.fr (B. Belaroussi).
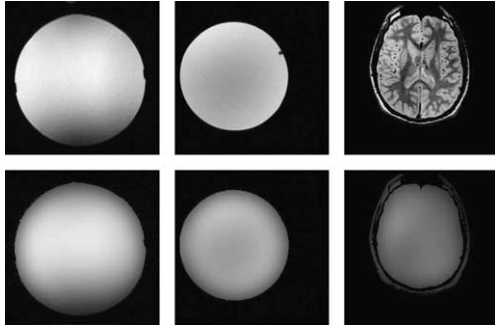
Fig. 1. Examples of MR images affected by intensity non-uniformity. First row shows the original images, second row shows the bias fields estimated using Milles et al. (2004). From left to right: homogeneous phantom acquired with a surface coil, homogeneous phantom acquired with a head coil and brain acquired with a head coil.

device, a pulse sequence and an object, all of them being possible sources for this artifact. Physical limitations of the imaging device can lead to flip angle variations. A first possibility is a non-uniform B_0 static field. Even though local variations of B_0 are partly compensated by shim tuning, they can lead to a local deformation of the imaging plane. It translates in both non-anatomical intensity variations and object distortion in the images (Bridcut et al., 2001). RF coil homogeneity, which depends on their geometrical and physical properties (Liang and Lauterbur, 2000), can also have an influence as shown by typical sensitivity problems that come up with the use of surface coils (Axel et al., 1987; Condon et al., 1987). Homogeneity problems are, however, not limited to surface coils (Collins et al., 1997; Collins and Smith, 2001). Gradient fields can also influence images, either due to their possible non-linearity, which leads to geometrical distortions (Langlois et al., 1999), or due to their switching that can trigger eddy currents. Problems can also arise with the amplifiers and digital-analogic converters (Wicks et al., 1993) or with the coil tuning itself (Simmons et al., 1994).

Intensity non-uniformity can be observed with both spin echo (Simmons et al., 1994; Barker et al., 1998) and gradient echo (Mihara et al., 1998; Reeder et al., 1998) pulse sequences. Spin Echo pulse sequences have been studied in-depth (Simmons et al., 1994). For this acquisition sequence, it appears that some parameters of the acquisition sequence, for example whether or not slices are interleaved, have a direct effect on the artifact magnitude. Interleaved acquisitions show to be far less affected by intensity non-uniformity. The repetition time (TR) and the number of echoes also have an effect on image quality. The TR influence can be understood by the triggering of eddy currents inside the imaged object when gradients are switching too rapidly. Number of echoes can affect image quality as refocusing can be altered after a large number of echoes.

Finally, interactions between the imaged object and the acquisition device can not be neglected (Woods and Henkelman, 1985). The shape of the imaged object has a significant effect on intensity non-uniformity, as well as on its electromagnetic properties (Sled and Pike, 1998). Such tissue-dependent properties have also been shown using samples from natural substances or human tissues (Alecci et al., 2001). They are the result of a combination of RF penetration and RF standing wave effects.

The model commonly used to describe corrupted data is a multiplicative model with additive noise:

$$v(\vec{r}) = g(\vec{r}) \cdot u(\vec{r}) + n(\vec{r}), \tag{1}$$

where $v(\vec{r})$ is the voxel intensity at location $\vec{r} = (x, y, z)$, $g(\vec{r})$ the corresponding value of the bias, or gain, field, $u(\vec{r})$ the true intensity spatial distribution and $n(\vec{r})$ an additive noise (Axel et al., 1987; Condon et al., 1987; Dawant et al., 1993; Meyer et al., 1995; Wells III et al., 1996). Spatial variations for g are supposed to be smooth and slow, u is considered as piecewise constant (Axel et al., 1987) and n has a Rician probability density distribution (Gudbjartsson and Patz, 1995). This model is consistent with RF field computation and mapping theory, which links pixel intensities with RF coil transmission and reception sensitivity (Insko and Bolinger, 1993; Barker et al., 1998). Intensity non-uniformity correction consists in determining u knowing v. This yields an underdetermined problem due to the fact that only $v(\vec{r})$ is known while both $g(\vec{r})$ and $u(\vec{r})$ have to be computed.

Intensity non-uniformity has been studied by the communities involved in the acquisition and the processing of MR data. Numerous methods have been proposed to suit their specific needs. MR physicists' goal is to improve acquired image quality by means of a better protocol. Image processing community's goal is to use a retrospective correction algorithm as a step to improve subsequent quantitative analysis. The purpose of this survey is not only to give an overview of existing methods available but also to bridge the gap between these two communities. We suggest a typology to sort them based on their location in the acquisition/processing pipeline. The two main categories are composed of prospective methods based on prior knowledge about acquisition parameters and retrospective image processing methods. Sorting is then refined based on the assumptions those methods rely on. Then, we present the validation protocols used to evaluate these different correction schemes both from a qualitative and quantitative point of view. Finally, a comparison of the methods, regarding their performance and applicability, is presented as well as information about the availability of intensity non-uniformity correction methods.

2. Prospective correction methods

Eq. (1) yields an ill-posed problem since neither bias field $g(\vec{r})$ nor true intensity $u(\vec{r})$ spatial distributions are known. Prior knowledge about either one of them can be obtained using a specially designed MR acquisition protocol. Intensity variations in MR data are due to the combined effect of the imaged object, the MR pulse sequence

and the imaging coils. Taking prior knowledge about some of these factors into account can ease intensity non-uniformity understanding and correction. The correction methods described in this section try to reduce the number of unknown factors involved. Two different approaches are proposed. The first approach consists of combining different datasets, by means of a mathematical model, to correct intensity variation observed on images. The second approach consists of trying to compensate unwanted flip angle variation during the acquisition process.

2.1. Multiple datasets combination

Prior knowledge can be obtained by combining data obtained from different datasets. The first strategy consists in using acquisition from a physical phantom whose physical properties and geometry are known. Remaining unknown factors are then coil and sequence properties. The second strategy consists in acquiring several datasets from the same object with different acquisition protocols. Influence of sequence or coil components is then separately evaluated.

2.1.1. Same imaging parameters, different objects

Acquisition of datasets from a homogeneous phantom provides insight on the object-dependent component (Sled and Pike, 1998). The acquired datasets are only affected by the sequence-dependent and coil-dependent components of intensity non-uniformity. Once the sequence parameters are set, the intensity non-uniformity of the acquired image is then directly related to the coil sensitivity which varies spatially with the MR signal in transmission and reception. To further reduce the influence of coils, the body coil, being more homogeneous than a surface coil, can be used as the transmitting coil. This gives a good representation of the receiving coil sensitivity variation when a uniform phantom is scanned (Axel et al., 1987). This representation leads to the gain field $g(\vec{r})$ defined in Eq. (1). This correction method has been used either directly (Axel et al., 1987; Condon et al., 1987) or via a mathematical representation of the bias field (Condon et al., 1987; Wicks et al., 1993). It can also be applied as a first step before further processing (Collewet et al., 2002). The main limitation in using a separate phantom acquisition is that the correction method does not take the influence of the object itself and its interaction with magnetic fields into account. This influence can be significantly non-linear (Wells III et al., 1996).

2.1.2. Same object, different imaging parameters

The combination of different datasets acquired from the same object allows removing the intensity non-uniformity artifact component linked to the object. A priori knowledge about the bias field can be obtained using different acquisition sequences or coils.

2.1.2.1. Same coil. The underlying assumption when using the same coil with different imaging parameters is that a

homogeneous tissue should be represented by a homogeneous intensity distribution. Any intensity variation in a given tissue class can be attributed to the bias field, and the corrupted data can be considered as a representation of the bias field spatial variations. This bias field information is used to correct datasets obtained with a different acquisition sequence. For example, a T2-weighted sequence can be corrected using the estimated bias field of a proton density (PD)-weighted sequence since the latter has an overall lower contrast (Liney et al., 1998).

For some pulse sequences, the relationship between flip angle and voxel intensity can be analytically computed. Using the obtained model, correction can be performed. From two Spin-Echo images obtained with two flip angles being, respectively, θ and 2θ, the spatial distribution of the flip angle is computed and used to compensate intensity non-uniformity (Mihara et al., 1998). Instead of using the same sequence with two different flip angles, it is also possible to estimate the flip angle spatial variation using a specific sequence, such as echo-planar imaging (EPI), and to use that information to correct data obtained using another pulse sequence (Thulborn et al., 1998).

2.1.2.2. Different coils. Different transmission and reception coils can be used in MRI, depending on the imaged object. These coils differ in their geometry, leading to different properties, and are usually sorted among surface or volume coils. Surface coils provide datasets with a good signal-to-noise ratio but a poor spatial uniformity. Acquisitions using a surface coil are thus corrupted by a more intense bias field compared to volume coils. Since body coils, which are volume coils, are assumed to have a uniform sensitivity, they can be chosen as references for correcting surface coil or phased-array coil data. Correction can be performed directly (Brey and Narayana, 1988) or through a statistical model solved using an optimization technique (Fan et al., 2003). Another solution is to use the pre-scan localization data to obtain prior knowledge about the bias field (Murakami et al., 1996). These pre-scan data can be acquired using either the body coil or a phased-array coil before every clinical protocol. A consequence of such multiple imaging techniques is an increased acquisition time.

2.2. Per-acquisition flip angle compensation

Methods described in this section rely on the assumption that the intensity non-uniformity artifact is mainly due to the RF coil. Those variations are compensated during the acquisition process.

A solution is to first estimate the sensitivity profile of a particular RF head coil along the z axis from both a network analyzer and in situ using the method described by Barker et al. (1998). Then a look-up table (LUT) is computed to correct these variations based on the estimated sensitivity profile. Finally, this LUT is used to actively modulate the transmitted RF power according to the slice position (Clare et al., 2001).

Another solution is to design a specific RF excitation pulse, based on two spatially independent terms. This has been used for magnetization-prepared rapid gradient echo (MP-RAGE) sequences (Deichmann et al., 2002). It compensates unwanted flip angle variations in a head coil. The new pulse sequence parameters are obtained from measurements on volunteers using a fast low angle shot (FLASH) sequence.

3. Retrospective correction methods

Retrospective processing methods propose to correct MR images corrupted by the non-uniformity artifact with only a few assumptions regarding the acquisition process. Those methods are numerous and have been sorted according to the flowchart presented in Fig. 2.

3.1. Using grayscale spatial distribution

Algorithms based on grayscale spatial distribution rely on the assumption that the variation of the artifact is spatially smooth and slowly varying across the image and that the ideal image is piecewise constant. This leads to different solutions, focusing either on the assumptions concerning the artefact or the true image.

3.1.1. Surface fitting

Surface fitting is an important type of interpolation in many applications. The aim of surface fitting is to fit a set of data points, as closely as possible with a specified surface as smooth as possible and flexible enough to provide a good approximation to the image brightness function. Since intensity non-uniformity is supposed to be smooth, it can be approximated by a smooth surface. Correction is done by dividing voxel-by-voxel the original image by the computed surfaces. The main difference between those methods is the basis functions used. They are chosen to be smooth, according to the assumptions mentioned above, which leads to two main basis function families: Spline and polynomial functions.

3.1.1.1. Spline basis functions. The different algorithms using spline basis functions vary in the way the fitting is performed. This fitting can require either a single pass or multiple passes.

Single pass fitting is based on a set of control points. This set can be obtained using a semi-automatic framework by requesting the user to select typical points in each tissue compartment. Another solution is to automatically select control points using a classifier (Dawant et al., 1993). For this automatic control points selection one can also use centers of mass extracted from 3×3 neighborhoods, instead of using single voxels (Zijdenbos et al., 1995).

Multiple pass fitting is based on minimizing an energy function. Fitting can be combined with segmentation steps in an iterative framework to correct images in which a tissue class is dominant (Gilles et al., 1996). Another solution is to choose a deformable surface framework for determining spline parameters by minimizing an energy function (Lai and Fang, 1999).

3.1.1.2. Polynomial basis functions. Using polynomial basis functions raises the same issues as using spline basis functions. For single pass computation, a physical phantom can be used to determine the surface's parameters, that will be used to correct other data (Tincher et al., 1993). This method has been further developed by using a segmented dataset instead of a phantom for parameters computation (Meyer et al., 1995).

Multiple pass fitting has also been studied to compute Legendre polynomials' coefficients by minimizing an
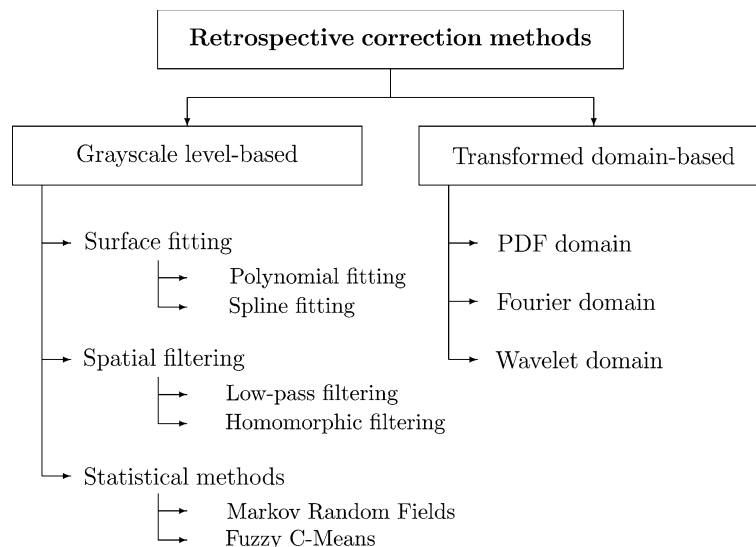

Fig. 2. Retrospective correction methods types.

energy function (Brechbuhler et al., 1996; Styner et al., 2000; Samsonov et al., 2002).

3.1.2. Spatial filtering

Methods based on a spatial filtering of the corrupted MR dataset use the assumption that the bias field consists of a low spatial frequency intensity variation. These correction algorithms first extract the intensity non-uniformity from the original data and then perform a voxel-by-voxel division between original data and the extracted intensity non-uniformity. The main difference between various spatial filtering methods is the filter type used in the extraction step. The filters used can be either low-pass or homomorphic filters.

3.1.2.1. Low-pass filtering. Low-pass filtering methods can be subdivided depending on the way intensity non-uniformity is extracted. This extraction can be performed using a single processing step or multiple processing steps. Single step methods are based on a median filter (Lim and Pfefferbaum, 1989; Harris et al., 1994; Narayana and Borthakur, 1995). The filtered dataset is considered as a representation of the intensity non-uniformity artifact.

Multiple processing step methods are based on two steps, at least one of them being a filtering step. Other steps can consist of extracting regions of small intensity variations using either an average or a median filter (Koivula et al., 1997). Extracted regions are then smoothed using a gaussian filter. Data obtained after using an average filter can be combined with information from the original data to obtain an estimate of intensity non-uniformity (Zhou et al., 2001). Another solution is to remove the edges by low-pass filtering applied on a gradient image. The obtained smoothed gradient image is then integrated to reconstruct the bias field (Vokurka et al., 1999).

3.1.2.2. Homomorphic filtering. Homomorphic filtering is a non-linear filtering technique used for image enhancement or correction (Gonzales and Woods, 1992). It simultaneously increases contrast and normalizes brightness. It can be performed with a low-pass filter, allowing to extract an estimate of the bias field (Johnston et al., 1996). Such a filter can be based on median or average kernels. The latter kernel proved to be more efficient for intensity non-uniformity correction (Brinkmann et al., 1998).

3.1.3. Statistical methods

Statistical methods described in this section mainly aim at segmenting datasets. However, they are designed to take intensity non-uniformity into account. Segmentation is achieved by means of maximum likelihood (ML)- and maximum a posteriori (MAP)-based methods or by Fuzzy-C-Means-based methods.

3.1.3.1. ML- and MAP-based methods. These methods label pixels according to probability values, which are determined based on the intensity distribution of the image. This estimation problem is based on a criterion which can be maximum a posteriori (MAP) (Wells III et al., 1996; Guillemaud and Brady, 1997; Rajapakse and Kruggel, 1998) or maximum likelihood (ML) (Van Leemput et al., 1999; Pham and Prince, 1999c; Prima et al., 2001; Zhang et al., 2001). Before the criterion can be assessed, the density function of the pixel intensity has to be modeled. Finite mixture (FM) (Van Leemput et al., 1999) and finite Gaussian mixture (FGM) models (Wells III et al., 1996) can be used. FM models are intrinsically limited since spatial information is not taken into account, pixels values being considered independent. To address this problem, a hidden Markov random field (HMRF) model can be used (Zhang et al., 2001). In this model, the spatial information in an image is encoded through contextual constraints of neighboring pixels. Those are expected to have the same class labels or similar intensities. Once the statistical criterion and the image model have been chosen, the model parameters must be estimated. Parameters estimation can be achieved using, for example, an expectation-maximization (EM) algorithm. The expectation step is equivalent to compute the posterior tissue class probabilities when the bias field is known while the maximization step is equivalent to a MAP estimator of the bias field when the tissue probabilities are known. EM was first used for brain images segmentation (Wells III et al., 1996) using an FGM model and a MAP-based approach. To take into account the pixels in the expected tissue classes, an outlier class with a non-Gaussian probability distribution can be introduced (Guillemaud and Brady, 1997). A MAP-based approach is also used in this method.

EM algorithms have also been extended to a more general framework with the expectation/conditional maximization (ECM) algorithm (Van Leemput et al., 1999; Prima et al., 2001) and the adaptative generalized EM (AGEM) algorithm (Pham and Prince, 1999c). Methods described by Van Leemput et al. (1999) and Prima et al. (2001) are similar. Each tissue class is modeled by a Normal distribution and the bias field is modeled as a linear combination of smooth fourth-order polynomial basis functions. The algorithm initialization is performed using a digital brain atlas with a priori probability maps for each tissue class. These methods use a ML-based approach. Optimization of the ML criterion can be based on a classic EM algorithm (Prima et al., 2001).

For T1-weighted images, a locally adaptive algorithm based on minimization of the classification error rates between different cerebral tissues has been proposed in Gispert et al. (2004). At each EM iteration, the classification thresholds that yield the minimum error rate are calculated. EM algorithm stops when the computed thresholds do not change between subsequent iterations.

Parameters of the model can also be estimated by a genetic algorithm. Genetic algorithms are a class of robust stochastic search and optimization procedures based on the Darwinian theory of evolution. Their basic principles were first introduced by Holland (1962) and their tuning relies

on a proper selection of only a few parameter values. They are well suited for estimating the parameters of mixtures of different distributions (Schroeter et al., 1998). This method is based on ML approach.

Finally, model parameters can be estimated with the iterative conditional modes (ICM) method. ICM is a deterministic algorithm which sequentially maximizes local conditional probabilities (Besag, 1986). ICM was first used in Rajapakse and Kruggel (1998). In this method, a HMRF model is used in combination with a MAP-based approach. Spatial dependence between neighboring pixels can be modeled using a Gaussion mixture model combined with Markov random fields (GMM–MRF) with a penalized ML approach (Kim et al., 2003). Parameters estimation is done using ECM algorithm. However, the E-step of the ECM algorithm is approximated by a fractional weight version of the ICM algorithm.

3.1.3.2. Fuzzy-C-Means based methods.
Fuzzy-C-Means (FCM) has been successfully used for segmenting of MR datasets (Bezdek, 1981). It clusters data by computing a measure membership, called the fuzzy membership, at each voxel for a specified number of classes. FCM is formulated as the minimization of an objective function. However, FCM is not appropriate for data corrupted by intensity inhomogeneity.

An extension of FCM has been proposed to take intensity non-uniformity into account (Lee and Vannier, 1996), by adapting the clustering to local variations. The original dataset is separated into two classes: soft tissue and outliers. For the soft tissue class, intensity non-uniformity is taken into account by using local means instead of a global mean. These means are then smoothed with a 3-D gaussian low-pass filter. A local signal amplitude map is obtained for each slice. This map is used to estimate gain field in this same slice. A corrected dataset is obtained by dividing the original dataset by the gain field previously estimated.

Pham and Prince (1999b,c) proposed an adaptive FCM (AFCM) scheme. Intensity non-uniformity is considered by multiplying the centroids by a gain field. Then, two regularization terms are added to the modified objective function to ensure that the gain field is smooth and slowly varying.

Recently, a modified FCM (MFCM) algorithm has been presented (Ahmed et al., 2002). The original FCM objective function is modified by adding a constraint term to compensate the intensity inhomogeneity and to allow the labeling of a voxel to be influenced by the labels in its immediate neighborhood. The constrained optimization is solved using the Lagrange multipliers technique.

3.2. Transformed domain-based methods

Instead of working in the spatial domain, correction can be performed in other domains that can be either dual, such as Fourier or wavelet domains, or complementary, such as the probability density functions (PDF) domain. Such domains allow different uses of the assumptions made on intensity non-uniformity. Once data are corrected, they are transformed back to the spatial domain.

3.2.1. PDF domain
Once PDF computation has been performed, the original intensity spatial distribution becomes an intensity probability distribution or histogram. In this domain, the intensity non-uniformity can be considered as a parasitic convolution term, which smooths the real intensity distribution and thus increases entropy. The PDF associated to the artifact can be modeled as a centered gaussian distribution. It then becomes possible to iteratively deconvolve the original histogram with the gaussian PDF modeling the artifact. The data are considered as corrected once there are no more significant variations between two consecutive iterations. A lookup table is computed between the corrupted and corrected PDFs, which will be applied on the original data to correct them (Sled et al., 1998).

The same histogram assumptions are used in Mangin (2000), Likar et al. (2001), Solanas and Thiran (2001) and Milles et al. (2004), but they are translated in an entropy minimization framework. The intensity non-uniformity is modeled using polynomial functions and a minimization is performed using Powell's method (Mangin, 2000; Likar et al., 2001). An extension of Likar et al. (2001) has been proposed in Solanas and Thiran (2001). This method exploited the fact that neighboring pixels are highly correlated. The full spatial information can also be integrated in the entropy minimization framework (Milles et al., 2004). In the method proposed by Vovk et al. (2004a,b), the intensity image features are computed using spatial image features using second derivatives. The main property of the second derivative is the ability to reduce cluster overlap.

3.2.2. Fourier domain
The methods presented here are an alternative to those described in Section 3.1.2. Both approaches deal with the original dataset filtering but differ in the domain where filters are built and applied. Filtering in Fourier domain has been seldom used for correcting intensity non-uniformity. The only filters applied are low-pass gaussian filters (Wald et al., 1995; Cohen et al., 2000).

3.2.3. Wavelet domain
The use of discrete wavelet transform (DWT) to correct for intensity non-uniformity has been proposed recently (Han et al., 2001; Lin et al., 2003). DWT decomposes the image into a cascade of orthogonal approximation and detail subspaces for different spatial resolutions. Each approximation subspace contains low-frequency information whereas the corresponding detail subspace contains high-frequency information. The original image can be reconstructed by combining those subimages. Since intensity non-uniformity consists of low frequencies, it can be estimated and corrected in the approximation subspaces.

Relevant subspaces can be computed either based on subspaces coefficients (Han et al., 2001) or based on the reconstructed image (Lin et al., 2003).

4. Evaluation tools for intensity non-uniformity correction methods

As stated in Sections 2 and 3, numerous methods, based on different theoretical backgrounds and approaches, have been developed to correct for the intensity inhomogeneity. However, a crucial point is to determine which method is the best for a given acquisition protocol. This implies the use of an evaluation framework, which can be either qualitative or quantitative, to compare the different correction approaches. Such a comparison has been proposed for blind correction methods (Arnold et al., 2001) or MR brain images correction (Velthuizen et al., 1998).

An objective evaluation framework is the combination of a ground truth and a quality control of the result. Ground truth consists of a prior knowledge about datasets used. We present in Section 4.1 the main solutions to obtain this prior knowledge. The quality control of the corrected data can be either qualitative, see Section 4.2.1, or quantitative, as described in Section 4.2.2. Finally, the different validation methodologies used for correction algorithms are summed up in Table 1.

4.1. Typical dataset used for validation

As stated before, an objective validation method may require a ground truth, based on strong prior knowledge about the real structure of the object of interest. However, alternative methods, such as the STAPLE method (Warfield et al., 2004), can be used. For datasets acquired in clinical situation, this ground truth is usually incomplete, leading to a subjective quality assessment. Consequently, other solutions have been proposed for validation purpose, leading to the use of numerical data, either synthetic or simulated, or the acquisition of images of physical phantoms with known characteristics.

4.1.1. Numerical datasets

Numerical datasets are commonly used for validation because of the ideal prior knowledge they provide. They allow both qualitative and quantitative evaluation. Typical numerical datasets are either synthetic or simulated.

4.1.1.1. Synthetic datasets. These datasets carry no realistic anatomical or physical information. They are usually used as a first step for objectively evaluating an image processing method (Wells III et al., 1996), their characteristics being already known.

4.1.1.2. Numerically simulated datasets. Since a synthetic dataset does not have realistic behavior, realisticly simulated datasets have become necessary. With the increase in computational power, such realistic datasets can be simulated. As an example, the interface *BrainWeb* developed by McGill University (Montréal, Canada) provides simulated brain MR datasets for various acquisition sequences and intensity non-uniformity levels (Collins et al., 1998).

4.1.2. Real datasets

The crucial point here is that ground truth is lacking when imaging organs in vivo, leading to a technical difficulty for quality assessment. Two possibilities have been considered to obtain prior knowledge about the object being imaged. The first solution is to image physical phantoms (Mihara et al., 1998), the second is to image real organs in vivo and to rely on experts knowledge for quality assessment (Rajapakse and Kruggel, 1998). Imaging objects such as physical phantoms increase knowledge about their structural and physical properties, even if those properties do not reflect the exact clinical reality. However, such physical phantom are not realistic enough.

In vivo data characteristics correspond to those of real clinical acquisitions. However, we lack prior knowledge about the structural and the physical properties of the imaged objects. This problem can be partially solved by relying on manual or semi-automated segmentations performed by medical experts (Wells III et al., 1996). This

Table 1
Overview of validation methods

Qualitative evaluation	
Profile	Ahmed et al. (1999), Cohen et al. (2000), Johnston et al. (1996), Lai and Fang (1999), Lee and Vannier (1996), Mihara et al. (1998), Sled et al. (1998), Vokurka et al. (1999), Wald et al. (1995)
Image	Ahmed et al. (1999), Axel et al. (1987), Brey and Narayana (1988), Clare et al. (2001), Collewet et al. (2002), Deichmann et al. (2002), Gilles et al. (1996), Lai and Fang (1999), Liney et al. (1998), Murakami et al. (1996), Sled et al. (1998), Thulborn et al. (1998), Wald et al. (1995), Wells III et al. (1996), Zhang et al. (2001)
Histogram	Clare et al. (2001), Collewet et al. (2002), Schroeter et al. (1998), Thulborn et al. (1998), Vokurka et al. (1999)
Quantitative evaluation	
Grayscale level	Brinkmann et al. (1998), Condon et al. (1987), Han et al. (2001), Koivula et al. (1997), Prima et al. (2001), Tincher et al. (1993), Wicks et al. (1993)
Segmented data	Dawant et al. (1993), Guillemaud and Brady (1997), Harris et al. (1994), Johnston et al. (1996), Lee and Vannier (1996), Likar et al. (2001), Meyer et al. (1995), Narayana and Borthakur (1995), Pham and Prince (1999a), Rajapakse and Kruggel (1998), Shattuck et al. (2001), Styner et al. (2000), Van Leemput et al. (1999), Vokurka et al. (1999), Wells III et al. (1996), Zhou et al. (2001), Zijdenbos et al. (1995)

can lead to databases like the *Internet Brain Segmentation Repository* (IBSR).[1] Nevertheless, using such user-driven segmentations as ground truth raises the problem of reproducibility of segmentation. Indeed, intra- and inter-operator variations can actually hamper the evaluation process.

4.2. Evaluation criteria

Evaluation is an important step towards the validation of correction methods. It can consist of qualitative or quantitative assessment of the corrected data in regard of the reference data.

4.2.1. Qualitative approaches

Qualitative evaluation is based on visual comparison of representations of reference and corrected datasets. Those representations are usually taken in the spatial domain, leading to images or profiles, or in the PDF domain, providing graylevel histograms.

4.2.1.1. Spatial domain. Visual evaluation in the spatial domain is commonly taken as a first step in the validation process as it is the most intuitive representation. When comparing images, the main criterion used is overall homogeneity inside each tissue compartment. This can be extended to profiles, where the operator looks for the piecewise constant aspect of those tissue compartments (Zhou et al., 2001).

4.2.1.2. PDF domain. An evaluation in the PDF domain can be less intuitive than in the spatial domain. It is rarely used when dealing with objects other than simple phantoms as the interpretation of histograms is almost impossible for complex objects. The typical criterion used is the graylevel spreading around main peaks. Sharper peaks mean that the different tissue classes are better separated (Vokurka et al., 1999).

4.2.2. Quantitative approaches

Quantitative validation is based on the evaluation of parameters considered to be significant. Quantitative measurements require a quantitative representation of the corrected dataset. Measurements can be separated in two types. The first one is an assessment of the variations of grayscale levels for a given tissue, or adjacent tissue compartments (Meyer et al., 1995). The second one is an assessment of the segmentation accuracy (Styner et al., 2000).

4.2.2.1. Grayscale level variations. A common assumption about MR data is that the spatial intensity distribution is piecewise constant and that each tissue corresponds to a unique grayscale level. Based on those hypothesis, a valid correction method should lessen the standard deviation in intensity for each tissue. The ratio between the standard deviation σ and the mean μ of a given tissue defines the coefficient of variation (CV), also called percentage of

in-slice non-uniformity (Wicks et al., 1993; Dawant et al., 1993; Sled, 1997):

$$CV = \frac{\sigma}{\mu}. \tag{2}$$

This parameter can be modified to measure the overlap between two tissue distributions t_1 and t_2 leading to the coefficient of joint variations (CJV) defined in Likar et al. (2000):

$$CJV(t_1, t_2) = \frac{\sigma(t_1) + \sigma(t_2)}{\mu(t_1) - \mu(t_2)}. \tag{3}$$

4.2.2.2. Information measurement. Another assumption is that intensity non-uniformity raises entropy of the data's histogram. Given a set of N graylevel measurements g_a and its associated probabilities $P(g_a)$, the entropy H is defined by:

$$H = -\sum_{a=1}^{N} P(g_a) \log P(g_a). \tag{4}$$

H is maximum when graylevel distribution is uniform. The scale invariant information measure can be derived from the standard entropy, defined by Eq. (4) (Thacker et al., 2002). In its continuous form, this measure is given by:

$$L = \sum_{a=1}^{n} \sqrt{\frac{P(g_a)}{g_a}}. \tag{5}$$

Whatever the used measure, the correction process should lower entropy.

4.2.2.3. Segmentation accuracy. Another solution to evaluate a correction algorithm is to assess for the accuracy of segmentation results before and after correction. Many statistical measurements are available, such as detection rates and similarity index (Styner et al., 2000; Zijdenbos et al., 1995). Detection rates provide information about correctly classified (true positive) and misclassified voxels (false positive and false negative). Correct detection rate (CDR) and incorrect detection rate (IDR) are defined by:

$$\begin{aligned} CDR &= \frac{N_{TP}}{N_1}, \\ IDR &= \frac{N_{FP} + N_{FN}}{N_1}, \end{aligned} \tag{6}$$

where N_1 is the number of voxels in the reference segmentation, N_{TP}, N_{FP}, N_{FN} are, respectively, the number of true positive, false positive and false negative voxels in the obtained segmentation.

A more sophisticated statistical measurement is given by the similarity index S defined as (Zijdenbos et al., 1995):

$$S = 2 \frac{n(A_a \bigcap A_b)}{n(A_a) + n(A_b)}, \tag{7}$$

where A_b, A_a are, respectively, the set of voxels in a given tissue class A before and after correction and $n(A)$ is the number of voxels in the class A.

---

[1] http://www.cma.mgh.harvard.edu/ibsr/.

Table 2
URL of correction algorithms available on the Internet

References	Operating system	URL
Sled et al. (1998)	Linux	http://www.bic.mni.mcgill.ca/software/N3/
Ashburner and Friston (1998)	Windows/Linux	http://www.fil.ion.ucl.ac.uk/spm/software/
Cohen et al. (2000)	MacOS/Linux	http://airto.bmap.ucla.edu/BMCweb/SharedCode/EQ/
Zhang et al. (2001)	Linux	http://www.fmrib.ox.ac.uk/analysis/research/fast/
Styner et al. (2000)	Win/MacOS/Linux	http://www.itk.org/HTML/MRIBiasCorrection.htm
Van Leemput et al. (1999)	Windows/Linux	http://www.medicalimagecomputing.com/EMS/
Shattuck et al. (2001)	Win/Linux/UNIX	http://neuroimage.usc.edu/brainsuite/

5. Comparison of correction methods

In the previous sections, we have presented the different intensity non-uniformity correction methods as well as the tools to validate them. The aim of this section is to introduce the contexts in which those methods have been used. Availability of the main correction methods is also presented (see Table 2).

5.1. Context of the proposed methods

From the literature, we summarized information about the general context on which correction methods have been proposed. We focus on the MR sequence used, the reception coil, the main static field intensity and the imaged object. Obtained results are given in Table 3. From this table, we can note that intensity non-uniformity concerns the three MR sequence families, i.e., SE, GE and EPI. Table 3 furthermore shows that correction is necessary both for images obtained with a surface coil and for images obtained with a head coil. Finally, many imaged objects, such as a homogeneous phantom, a brain, a breast, a wrist or a prostate are affected by the artefact. Hence, intensity non-uniformity can be attributed to a combination of the following three parameters, as described in Section 1: object, coil and MR sequence. It is interesting to note that most of the proposed correction algorithms are dedicated to brain images, showing their specificity and consequently, their limitations. However, intensity non-uniformity correction is also needed for acquisitions involving surface coils, e.g., spine or thoracic MRI.

5.2. Availability of the main algorithms

The main correction algorithms used today are available on the web site of their author, see Table 2. Hence, they can be downloaded and tested for the desired application. Most of the correction methods, which are Windows and Linux compatible, are generally included in image processing software packages. They can be specific to MRI, such as SPM[2] and FSL-FMRIB,[3] or more general such as ITK.[4]

5.3. Quantitative comparison of the proposed methods

Even if it is not the aim of this survey, it is important to know which correction algorithm can be considered as the most efficient for a given context. Such a work has been recently published for post-processing based methods (Velthuizen et al., 1998; Arnold et al., 2001).

The first study evaluates the efficiency of correction methods and their impact on tumor response measurements (Velthuizen et al., 1998). Results are summarized here. Four correction algorithms are compared: a phantom correction method (Wicks et al., 1993), an image smoothing technique (Narayana and Borthakur, 1995), homomorphic filtering (Johnston et al., 1996), and a surface fitting approach (Dawant et al., 1993).

The correction methods were tested on SE and FSE images acquired from six brain tumor cases using a 1.5T MR scanner. The efficiency of correction methods and their impact on tumor response measurements are measured. One important result is that the intensity non-uniformity is different for each correction method and each MR image. For smoothing and homomorphic techniques, the non-uniformity images are blurred versions of the original image, reflecting the tissue dependent brightness patterns. It means that the underlined hypothesis of spatial frequencies separation of the non-uniformity and the signal is not achieved. The aim of this study was to evaluate the impact of correction methods in brain tumor response measurements. However, even if correction is performed, no improvement in tumor segmentation was observed using any of the evaluated correction methods. This result is attributed to the fact that tumors are usually well localized.

A more complete study has been developed in Arnold et al. (2001), for a specific neuroscientific application. Six correction methods are tested: N3 (Sled et al., 1998), HUM (Brinkmann et al., 1998), EQ (Cohen et al., 2000), BFC (Shattuck et al., 2001), SPM (Ashburner and Friston, 1998), and CMA provided by the Center for Morphometric Analysis at the Massachusetts General Hospital. Test data consisted of simulated and real MR data volumes obtained at 1.5 and 3 T using 3D FLASH and 3D GRASS sequences. The correction methods evaluation consisted of a visual analysis of intensity histograms before and after correction. Furthermore, performances were evaluated on

---

[2] http://www.fil.ion.ucl.ac.uk/spm/.
[3] http://www.fmrib.ox.ac.uk/fsl/.
[4] http://www.itk.org/.

Table 3
Summary of the methods, information not available was termed N/A

References	Acquisition			
	Coil	Pulse sequences	Field	Objects
Ahmed et al. (1999, 2002)	N/A	N/A	1.5 T	Brain
Axel et al. (1987)	SC	SE	N/A	Wrist
Brey and Narayana (1988)	SC	N/A	2 T	Food/rabbit
Brinkmann et al. (1998)	SC	SPGR	N/A	Brain
Clare et al. (2001)	HC	EPI/SE	3 T	Brain
Cohen et al. (2000)	HC	GE/SE/SPGR	3 T	Brain
Collewet et al. (2002)	SC	SE	0.2 T	Fish
Condon et al. (1987)	SC	SE	0.15 T	Brain
Dawant et al. (1993)	HC	SE	1.5 T	Brain
Deichmann et al. (2002)	HC	MP-RAGE	2 T	Brain
Gilles et al. (1996)	SC	N/A	N/A	Breast
Guillemaud and Brady (1997)	HC/SC	SE	1.5 T	Brain/breast
Han et al. (2001)	SC	GE/SE	1.5 T	Brain/carotid
Harris et al. (1994)	HC	SE	1.5 T	Brain
Johnston et al. (1996)	HC	SE	1.5 T	Brain
Koivula et al. (1997)	BC/SC	SE	1 T	Brain/liver/spine
Lai and Fang (1999)	SC	N/A	N/A	Brain/breast/thorax
Lee and Vannier (1996)	HC/PA/SC	MP-RAGE	1.5 T	Brain
Likar et al. (2000, 2001)	HC/SC	GE/SE	1 T	Brain/breast
Liney et al. (1998)	SC	FSPGR/FSE	1.5 T	Prostate
Meyer et al. (1995)	BC/HC/SC	SE	0.35 T/1.5 T	Brain/breast/thorax
Mihara et al. (1998)	SC	GE	7 T	Phantom
Murakami et al. (1996)	PA/SC	GE/SE	1.5 T	Brain/spine
Narayana and Borthakur (1995)	HC	SE	1.5 T	Brain
Pham and Prince (1999b,c)	HC	SE	N/A	Brain
Pham and Prince (1999a)	HC	SE	N/A	Brain
Prima et al. (2001)	HC	GE	1.5 T	Brain
Rajapakse and Kruggel (1998)	HC	SPGR/FLASH	1.5 T	Brain
Schroeter et al. (1998)	HC	MP-RAGE	1.5 T	Brain
Sled et al. (1998)	HC	N/A	1.5 T	Brain
Thulborn et al. (1998)	SC	GE/EPI	1.5 T	Brain
Tincher et al. (1993)	BC	SE	0.5 T	Thorax
Shattuck et al. (2001)	N/A	N/A	1.5 T	Brain
Styner et al. (2000)	HC/SC	N/A	1.5 T	Brain/breast
Van Leemput et al. (1999)	HC	MP-RAGE	1.5 T	Brain
Vokurka et al. (1999)	HC/SC	FSE/SE/EPI	1.5 T	Brain/shoulder/spine
Wald et al. (1995)	PA	FSE/SPGR	1.5 T	Brain
Wells III et al. (1996)	HC/SC	GE/SE	1.5 T	Brain
Wicks et al. (1993)	HC/SC	SE	0.5 T	Brain
Zhang et al. (2001)	HC	N/A	N/A	Brain
Zhou et al. (2001)	HC	SE	0.5 T	Brain
Zijdenbos et al. (1995)	HC	N/A	N/A	Brain

the Montreal Brain Phantom with added known non-uniformity levels. Finally, real MR data volumes were used. For the real data, a voxel-based principal component analysis followed by a canonical variables analysis (PCA/VCA) was performed to determine the within-algorithm similarity and between-algorithm differences. The tighter the cluster of non-uniformity corrected volumes, the better the performance of the correction algorithm. The performance of a correction algorithm was also assessed by computing its stability, consisting of recursively applying each of algorithms to its corrected output volume for five iterations. At each iteration, the extracted bias field approaches to uniformity.

For phantom studies, N3 and BFC give the best results, indicating that the applied non-uniformity has been nearly completely removed. Histogram comparison of real data, before and after correction, indicates that the spm-corrected volume demonstrates a reduction in the height of gray-matter peak and a global shift of the white-matter peak to lower intensity values. An interesting result is the frequency content of the extracted non-uniformity image. N3, BFC, and SPM non-uniformity images have a low-frequency content while higher spatial frequencies, significantly influenced by the underlying brain anatomy, appears. The iteratively extracted N3 and BFC non-uniformity images rapidly approach a constant value, indicating their stability. EQ and CMA slowly converge while no appreciable change is observed for HUM. The erratic behavior of the SPM method is striking. Even if none of the tested algorithms performs well in all circumstances,

locally adaptive methods outperformed non-adaptive methods.

The outcome of studies comparing different algorithms for intensity non-uniformity correction is that none of the correction methods performs ideally in all cases, particularly considering that some methods are not robust when images show only little or no intensity non-uniformity effects. Locally adaptive methods seem to provide a more accurate correction than non-adaptive techniques, and thus suggest to be more efficient.

6. Conclusion

In this paper, we have considered intensity non-uniformity correction as a global problem involving multiple communities with different objectives. We have proposed an overview of all existing methods available and we have suggested an original typology to sort them based on the way correction is performed and on the assumptions made. This survey improves the understanding of the artifact correction and offers to any person from each community an upstream vision of the correction problem. From the surveyed literature, we separated correction methods into prospective and retrospective approaches with fine clustering in each category. Furthermore, we have presented validation protocols used to evaluate these different correction schemes both from a qualitative and a quantitative point of view. Finally, we have presented an overview of the contexts in which methods have been developed.

In conclusion, the fact that numerous methods have already been developed shows that the intensity non-uniformity artifact is not yet understood completely. The issue of correcting for intensity non-uniformity is still raised, but significant improvements for those methods could be met by studying this artifact's origins more thoroughly. This study could lead to a better model of this artifact, to a better correction algorithm and to a better validation protocol. Another issue could be a cooperative approach between the two communities to propose both a more robust correction method associated to an efficient evaluation scheme adapted to the context.

References

Ahmed, M., Yamany, S., Mohamed, N., Farag, A., Moriarty, T., 1999. Bias field estimation and adaptive segmentation of MRI data using a modified fuzzy C-means algorithm. In: International Symposium and Exhibition on Computer Assisted Radiology and Surgery (CARS '99). p. 1004.

Ahmed, M., Yamany, S., Mohamed, N., Farag, A., Moriarty, T., 2002. A modified fuzzy C-means algorithm for bias field estimation and segmentation of MRI data. IEEE Trans. Med. Imaging 21 (3), 193–199.

Alecci, M., Collins, C., Smith, M., Jezzard, P., 2001. Radio frequency magnetic field mapping of a 3 Tesla birdcage coil: experimental and theoretical dependence on sample properties. Magnet. Reson. Med. 46 (2), 379–385.

Arnold, J., Liow, J.-S., Schaper, K., Stern, J., Sled, J., Shattuck, D., Worth, A., Cohen, M., Leahy, R., Mazziotta, J., Rottenberg, D., 2001. Qualitative and quantitative evaluation of six algorithms for correcting intensity nonuniformity effects. NeuroImage 13 (5), 931–943.

Ashburner, J., Friston, K., 1998. MRI sensitivity correction and tissue classification. NeuroImage 7 (4), S107.

Axel, L., Constantini, J., Listerud, J., 1987. Intensity correction in surface-coil MR imaging. Am. J. Roentgenol. 148, 418–420.

Barker, G., Simmons, A., Arridge, S., Tofts, P., 1998. A simple method for investigating the effects of non-uniformity of radiofrequency transmission and radiofrequency reception in MRI. Brit. J. Radiol. 71 (841), 59–67.

Bellon, E., Haacke, E., Coleman, P., Sacco, D., Steiger, D., Gangarosa, R., 1986. MR artifacts: a review. Am. J. Roentgenol. 147, 1271–1281.

Besag, J., 1986. On the statistical analysis of dirty pictures. J. Roy. Stat. Soc. B Met. 48 (3), 259–302.

Bezdek, J., 1981. Pattern Recognition with Fuzzy Objective Function Algorithms. Plenum Press.

Brechbuhler, C., Gerig, G., Szekely, G., 1996. Compensation of spatial inhomogeneity in MRI based on a parametric field estimate. In: Visualisation in Biomedical Computation (VBC '96). pp. 141–146.

Brey, W., Narayana, P., 1988. Correction for intensity falloff in surface coil magnetic resonance imaging. Med. Phys. 15 (2), 241–245.

Bridcut, R., Redpath, T., Gray, C., Staff, R., 2001. The use of SPAMM to assess spatial distortion due to static field inhomogeneity in dental MRI. Phys. Med. Biol. 46 (5), 1357–1367.

Brinkmann, B., Manduca, A., Robb, R., 1998. Optimized homomorphic unsharp masking for MR grayscale inhomogeneity correction. IEEE Trans. Med. Imaging 17 (2), 161–171.

Clare, S., Alecci, M., Jezzard, P., 2001. Compensating for B1 inhomogeneity using active transmit power modulation. Magn. Reson. Imaging 19 (10), 1349–1352.

Cohen, M., DuBois, R., Zeineh, M., 2000. Rapid and effective correction of RF inhomogeneity for high field magnetic resonance imaging. Hum. Brain Mapp. 10 (4), 204–211.

Collewet, G., Davenel, A., Toussaint, C., Akoka, S., 2002. Correction of intensity nonuniformity in Spin-Echo T1-weighted images. Magn. Reson. Imaging 20 (4), 365–373.

Collins, C., Smith, M., 2001. Calculations of B1 distribution, SNR, and SAR for a surface coil adjacent to an anatomically-accurate human body model. Magnet. Reson. Med. 45 (4), 692–699.

Collins, C., Li, S., Yang, Q., Smith, M., 1997. A method for accurate calculation of B1 fields in three dimensions. Effects of shield geometry on field strength and homogeneity in the birdcage coil. J. Magn. Reson. 125 (2), 233–241.

Collins, D., Zijdenbos, A., Kollokian, V., Sled, J., Kabani, N., Holmes, C., Evans, A., 1998. Design and construction of a realistic digital brain phantom. IEEE Trans. Med. Imaging 17 (3), 463–468.

Condon, B., Patterson, J., Wyper, D., Jenkins, A., Hadley, D., 1987. Image non-uniformity in magnetic resonance imaging: its magnitude and methods for its correction. Brit. J. Radiol. 60 (709), 83–87.

Dawant, B., Zijdenbos, A., Margolin, R., 1993. Correction of intensity variations in MR images for computer-aided tissue classification. IEEE Trans. Med. Imaging 12 (4), 770–781.

Deichmann, R., Good, C., Turner, R., 2002. RF inhomogeneity compensation in structural brain imaging. Magnet. Reson. Med. 47 (2), 398–402.

Fan, A., Wells, W., Fisher, J., Cetin, M., Haker, S., Mulkern, R., Tempany, C., Willsky, A., 2003. A unified variational approach to denoising and bias correction in MR. In: International Conference on Information Processing in Medical Imaging (IPMI '03). pp. 148–159.

Gilles, S., Brady, M., Declerck, J., Thirion, J.-P., Ayache, N., 1996. Bias field correction of breast MR images. In: Visualisation in Biomedical Computation (VBC '96). pp. 153–158.

Gispert, J., Reig, S., Pascau, J., Vaquero, J., Garca-Barreno, P., Desco, M., 2004. Method for bias field correction of brain T1-weighted magnetic resonance images minimizing segmentation error. Hum. Brain Mapp. 22 (2), 133–144.

Gonzales, R., Woods, R., 1992. Digital Image Processing. Prentice-Hall.

Gudbjartsson, H., Patz, S., 1995. The Rician distribution of noisy MRI data. Magnet. Reson. Med. 34 (6), 910–914.

Guillemaud, R., Brady, M., 1997. Estimating the bias field of MR images. IEEE Trans. Med. Imaging 16 (3), 238–251.

Han, C., Hatsukami, T., Yuan, C., 2001. A multi-scale method for automatic correction of intensity non-uniformity in MR images. J. Magn. Reson. Imaging 13 (3), 428–436.

Hanson, L., Dyrby, T., 2002. RF inhomogeneity correction: validity of the smooth-bias approximation. In: Int. Soc. Mag. Reson. Med. (ISMRM '02). p. 2316.

Harris, G., Barta, P., Peng, L., Lee, S., Brettschneider, P., Shah, A., Henderer, J., Schlaepfer, T., Pearlson, G., 1994. MR volume segmentation of gray matter and white matter using manual thresholding: dependence on image brightness. Am. J. Neuroradiol. 15 (2), 225–230.

Holland, J., 1962. Outline for a theory of adaptive systems. J. ACM 9 (3), 297–314.

Insko, E.K., Bolinger, L., 1993. Mapping of the radiofrequency field. J. Magn. Reson. Ser. A 103 (1), 82–85.

Johnston, B., Atkins, M., Mackiewich, B., Anderson, M., 1996. Segmentation of multiple sclerosis lesions in intensity corrected multispectral MRI. IEEE Trans. Med. Imaging 15 (2), 154–169.

Kim, S.-G., Ng, S.-K., McLachlan, G., Wang, D., 2003. Segmentation of brain MR images with bias field correction. In: Workshop on Digital Image Computing. pp. 3–8.

Koivula, A., Alakuuala, J., Tervonen, O., 1997. Image feature based automatic correction of low-frequency spatial intensity variations in MR images. Magn. Reson. Imaging 15 (10), 1167–1175.

Lai, S.-H., Fang, M., 1999. A new variational shape-from-orientation approach to correcting intensity inhomogeneities in magnetic resonance images. Med. Image Anal. 3 (4), 409–424.

Langlois, S., Desvignes, M., Constans, J., Revenu, M., 1999. MRI geometric distorsion: a simple approach to correcting the effects of non-linear gradient fields. J. Magn. Reson. Imaging 9 (6), 821–831.

Lee, S., Vannier, M., 1996. Post-acquisition correction of MR inhomogeneities. Magnet. Reson. Med. 36 (2), 275–286.

Liang, Z.-P., Lauterbur, P., 2000. Principles of Magnetic Resonance Imaging: A Signal Processing Perspective. IEEE Press.

Likar, B., Viergever, M., Pernus, F., 2000. Retrospective correction of MR intensity inhomogeneity by information minimization. In: International Conference on Medical Image Computing and Computer-Assisted Intervention (MICCAI '00). pp. 375–384.

Likar, B., Viergever, M., Pernus, F., 2001. Retrospective correction of MR Intensity in MR inhomogeneity by information minimization. IEEE Trans. Med. Imaging 20 (12), 1398–1410.

Lim, K., Pfefferbaum, A., 1989. Segmentation of MR brain images into cerebrospinal fluid spaces, white and gray matter. J. Comput. Assist. Tomo. 13 (4), 588–593.

Lin, F.-H., Chen, Y.-J., Belliveau, J., Wald, L., 2003. A wavelet-based approximation of surface coil sensitivity profiles for correction of image intensity inhomogeneity and parallel imaging reconstruction. Hum. Brain Mapp. 19 (2), 96–111.

Liney, G., Turnbull, L., Knowles, A., 1998. A simple method for the correction of endorectal surface coil inhomogeneity in prostate imaging. J. Magn. Reson. Imaging 8 (4), 994–997.

Mangin, J.-F., 2000. Entropy minimization for automatic correction of intensity nonuniformity. In: IEEE Workshop on Mathematical Methods in Biomedical Image Analysis (MMBIA '00). pp. 162–169.

Meyer, C., Bland, P., Pipe, J., 1995. Retrospective correction of intensity inhomogeneities in MRI. IEEE Trans. Med. Imaging 14 (1), 36–41.

Mihara, H., Iriguchi, N., Ueno, S., 1998. A method of RF inhomogeneity correction in MR imaging. Magn. Reson. Mater. Phys. 7 (2), 115–120.

Milles, J., Zhu, Y., Chen, N., Panych, L., Gimenez, G., Guttmann, C., 2004. MRI intensity nonuniformity correction using simultaneously spatial and gray-level histogram information. In: SPIE Medical Imaging. pp. 734–742.

Murakami, J., Hayes, C., Weinberger, E., 1996. Intensity correction of phased-array surface coil images. Magnet. Reson. Med. 35 (4), 585–590.

Narayana, P., Borthakur, A., 1995. Effect of radio frequency inhomogeneity correction on the reproducibility of intra-cranial volumes using MR image data. Magnet. Reson. Med. 33 (3), 396–400.

Pham, D., Prince, J., 1999. A generalized EM algorithm for robust segmentation of magnetic resonance images. In: Conference on Information Sciences and Systems (CISS '99). pp. 558–563.

Pham, D., Prince, J., 1999b. Adaptive fuzzy segmentation of magnetic resonance images. IEEE Trans. Med. Imaging 18 (9), 737–752.

Pham, D., Prince, J., 1999c. An adaptive fuzzy C-means algorithm for image segmentation in the presence of intensity inhomogeneities. Pattern Recogn. Lett. 20 (1), 57–68.

Prima, S., Ayache, N., Barrick, T., Roberts, N., 2001. Maximum likelihood estimation of the bias field in MR brain images: investigating different modelings of the imaging process. In: International. Conference on Medical Image Computing and Computer-Assisted Intervention (MICCAI '01). pp. 811–819.

Rajapakse, J., Kruggel, F., 1998. Segmentation of MR images with intensity inhomogeneities. Image Vision Comput. 16 (3), 165–180.

Reeder, S., Faranesh, A., Boxerman, J., McVeigh, E., 1998. In vivo measurement of T2* and field inhomogeneity maps in the human heart at 1.5 T. Magnet. Reson. Med. 39 (6), 988–998.

Samsonov, A., Whitaker, R., Kholmovski, E., Johnson, C., 2002. Parametric method for correction of intensity inhomogeneity in MRI data. In: Intl. Soc. Mag. Reson. Med. (ISMRM '02). p. 154.

Schroeter, P., Vesin, J.-M., Langenberger, T., Meuli, R., 1998. Robust parameter estimation of intensity distributions for brain magnetic resonance imaging. IEEE Trans. Med. Imaging 17 (2), 173–186.

Shattuck, D., Sandor-Leahy, S., Schaper, K., Rottenberg, D., Leahy, R., 2001. Magnetic resonance image tissue classification using a partial volume model. NeuroImage 13 (5), 856–876.

Simmons, A., Tofts, P., Barker, G., Arridge, S., 1994. Sources of intensity nonuniformity in spin echo images at 1.5 T. Magnet. Reson. Med. 32 (1), 121–128.

Sled, J.G., 1997. A non-parametric method for automatic correction of intensity non-uniformity in MRI data. Master's thesis, Department of Biomedical Engineering, McGill University, Montreal, Canada.

Sled, J., Pike, G., 1998. Standing-wave and RF penetration artifacts caused by elliptic geometry: an electrodynamic analysis of MRI. IEEE Trans. Med. Imaging 17 (4), 653–662.

Sled, J., Zijdenbos, A., Evans, A., 1998. A nonparametric method for automatic correction of intensity nonuniformity in MRI data. IEEE Trans. Med. Imaging 17 (1), 87–97.

Solanas, E., Thiran, J.-P., 2001. Exploiting voxel correlation for automated MRI bias field correction by conditional entropy minimization. In: International Conference on Medical Image Computing and Computer-Assisted Intervention (MICCAI '01). pp. 1220–1221.

Styner, M., Brechbuhler, C., Szekely, G., Gerig, G., 2000. Parametric estimate of intensity inhomogeneities applied to MRI. IEEE Trans. Med. Imaging 19 (3), 153–165.

Thacker, N., Lacey, A., Bromiley, P., 2002. Validating MRI field homogeneity correction using image information measures. In: British Machine Vision Conference (BMVC '02). pp. 626–635.

Thulborn, K., Boada, F., Shen, G., Christensen, J., Resse, T., 1998. Correction of B1 inhomogeneities using echo-planar imaging of water. Magnet. Reson. Med. 39 (3), 369–375.

Tincher, M., Meyer, R., Gupta, R., Williams, W., 1993. Polynomial modeling and reduction of RF body coil spatial inhomogeneity in MRI. IEEE Trans. Med. Imaging 12 (2), 361–365.

Van Leemput, K., Maes, F., Vandermeulen, D., Suetens, P., 1999. Automated model-based bias field correction of MR images of the brain. IEEE Trans. Med. Imaging 18 (10), 885–896.

Velthuizen, R., Heine, J., Cantor, A., Lin, H., Fletcher, L., Clarke, L., 1998. Review and evaluation of MRI nonuniformity corrections for brain tumor response measurements. Med. Phys. 25 (9), 1655–1666.

Vokurka, E., Thacker, N., Jackson, A., 1999. A fast model independent method for automatic correction of intensity nonuniformity in MRI data. J. Magn. Reson. Imaging 10 (4), 550–562.

Vovk, U., Pernus, F., Likar, B., 2004a. MRI intensity inhomogeneity correction by combining intensity and spatial information. Phys. Med. Biol. 49 (17), 4119–4133.

Vovk, U., Pernus, F., Likar, B., 2004. Multi-feature intensity inhomogeneity correction in MR images. In: International Conference on Medical Image Computing and Computer-Assisted Intervention (MICCAI '04). pp. 283–290.

Wald, L., Carvajal, L., Moyher, S., Nelson, S., Grant, P., Barkovich, A., Vigneron, D., 1995. Phased array detectors and an automated intensity-correction algorithm for high-resolution MR imaging of the human brain. Magnet. Reson. Med. 34 (3), 433–439.

Warfield, S., Zou, K., Wells, W., 2004. Simultaneous truth and performance level estimation (STAPLE): an algorithm for the validation of image segmentation. IEEE Trans. Med. Imaging 23 (7), 903–921.

Wells III, W., Grimson, W., Kikinis, R., Jolesz, F., 1996. Adaptative segmentation of MRI data. IEEE Trans. Med. Imaging 15 (4), 429–442.

Wicks, D., Barker, G., Tofts, P., 1993. Correction of intensity nonuniformity in MR images of any orientation. Magn. Reson. Imaging 11 (2), 183–196.

Woods, L., Henkelman, R., 1985. MR Image artifacts from periodic motion. Med. Phys. 12 (2), 143–151.

Zhang, Y., Brady, M., Smith, S., 2001. Segmentation of brain MR images through a hidden Markov random field model and the expectation-maximization algorithm. IEEE Trans. Med. Imaging 20 (1), 45–57.

Zhou, L., Zhu, Y., Bergot, C., Laval-Jeanet, A.-M., Bousson, V., Laredo, J.-D., Laval-Jeanet, M., 2001. A method of radio-frequency inhomogeneity correction for brain tissue segmentation in MRI. Comput. Med. Imag. Grap. 25 (5), 379–389.

Zijdenbos, A., Dawant, B., Margolin, R., 1995. Intensity correction and its effect on measurement variability in MRI. In: International Symposium and Exhibition on Computer Assisted Radiology and Surgery (CARS '95). pp. 216–221.